Weakly Coupled $s = 1/2$ Quantum Spin Singlets in $Ba_3Cr_2O_8$

M. Kofu,[1] J.-H. Kim,[1] S. Ji,[1,2] S.-H. Lee,[1] H. Ueda,[3] Y. Qiu,[2,4] H.-J. Kang,[2,4] M. A. Green,[2,4] and Y. Ueda[3]

[1]*Department of Physics, University of Virginia, Charlottesville, Virginia 22904-4714, USA*
[2]*NIST Center for Neutron Research, Gaithersburg, Maryland 20899-6100, USA*
[3]*Institute for Solid State Physics, University of Tokyo, Kashiwa 277-8581, Japan*
[4]*Department of Materials Science and Engineering, University of Maryland, College Park, Maryland 20742-6393, USA*

(Received 29 September 2008; revised manuscript received 24 November 2008; published 22 January 2009)

Using single crystal inelastic neutron scattering with and without the application of an external magnetic field and powder neutron diffraction, we have characterized magnetic interactions in $Ba_3Cr_2O_8$. Even without a field, we found that there exist three singlet-to-triplet excitation modes in the (h, h, l) scattering plane. Our complete analysis shows that the three modes are due to spatially anisotropic interdimer interactions that are induced by lattice distortions of the tetrahedron of oxygens surrounding the Jahn-Teller active $Cr^{5+}(3d^1)$. The strong intradimer coupling of $J_0 = 2.38(2)$ meV and weak interdimer interactions ($|J_{\text{inter}}| \leq 0.52(2)$ meV) makes $Ba_3Cr_2O_8$ a good model system for weakly coupled $s = 1/2$ quantum spin dimers.

DOI: 10.1103/PhysRevLett.102.037206 PACS numbers: 75.10.Jm, 75.25.+z

For the past two decades, the field of quantum magnets has provided a number of new exotic collective phenomena [1]. Progress has always been moderated by the availability of suitable spin 1/2 materials with distinct structural motifs. The ubiquitous $Cu^{2+}(3d^9, s = 1/2)$ ion is often relied upon as the platform for new materials design. Magnetic-field-induced quantum phase transitions are a typical example. The field-induced condensation of magnons has been experimentally observed in coupled quantum ($s = 1/2$) dimer systems based on Cu^{2+} ions, such as $TlCuCl_3$ [2–4] and $BaCuSi_2O_6$ [5], which are adequately described by the Bose-Einstein condensation theory [2,6,7]. However, the robustness of such descriptions can only be truly evaluated with investigation into complementary materials. This calls for finding other good model systems of quantum dimers, especially based on non-Cu^{2+} ions.

Recently, a new class of spin dimer systems has been reported with the general formula $A_3B_2O_8$ [8–11], where A is an alkaline earth metal such as Ba^{2+} or Sr^{2+} and B is a 5+ transition metal ion that forms dimers along the c axis [see Fig. 1(b)]. Interestingly, a frustrating triangular lattice is formed by the dimers in the ab plane [see Fig. 1(a)] [8]. For $Ba_3Mn_2O_8$ with orbitally nondegenerate $Mn^{5+}(3d^2, s = 1)$, specific heat measurements under H provide experimental evidence of a condensation of magnons [9]. A recent inelastic neutron scattering study showed that the magnetic interactions between dimers in $Ba_3Mn_2O_8$ are effectively two-dimensional in nature as a result of this interplane frustration [12]. More recently, the related chromate $(Ba, Sr)_3Cr_2O_8$ with the quantum ($s = 1/2$) spin from the orbitally degenerate $Cr^{5+}(3d^1; s = 1/2)$ ion has been synthesized [10,11]. These compositions do not exhibit long-range order above 1.5 K, and their bulk susceptibility data at low temperatures observe the quantum dimer model. The application of an external magnetic field at 1.6 K rapidly increases the bulk magnetization in $Ba_3Cr_2O_8$ above $H_{c1} \simeq 12$ T to its saturation value at $H_{c1} \approx 23$ T [10]. In contrast to the manganate, no magnetization plateau was observed.

Here we report our inelastic neutron scattering data obtained from single crystals of $Ba_3Cr_2O_8$ with and without application of an external magnetic field. We have found that at 1.7 K, even without a field, there are three singlet-to-triplet excitation modes in (h, h, l) directions, which contrasts with the single mode observed in $Ba_3Mn_2O_8$. Our analysis shows that the three modes come from spatially anisotropic interdimer interactions in three different crystal domains. We also show by neutron

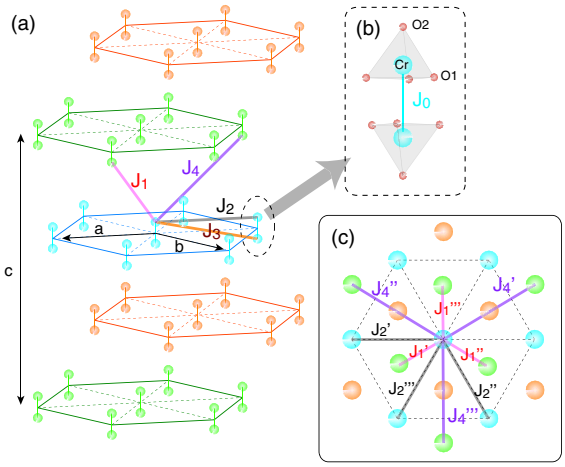

FIG. 1 (color online). Schematic diagram of the crystal structure of $Ba_3Cr_2O_8$ that shows (a) the triangular network of Cr^{5+} dimers in the ab plane and their relative stacking along the c axis in an $ABCABC$ arrangement. (b) Two oriented Cr^{5+} tetrahedra bound with four oxygen (O^{2-}) ions to afford the Cr^{5+} dimer arrangement with magnetic exchange, J_0, which is at a distance of $d_0 = 3.97$ Å. (c) The ab-plane projection of the Cr^{5+} ions, showing the alternative exchange pathways.

diffraction measurements that the spatial anisotropy in $Ba_3Cr_2O_8$ is due to a structural transition from rhombohedral $R\bar{3}m$ to monoclinic $C2/c$ symmetry below 70 K that is induced by the orbital degeneracy of the Cr^{5+} ($3d^1$) ion. Our analysis of dispersions of the singlet-to-triplet excitations shows that this system is an excellent model system for three-dimensional weakly coupled dimers with dominant intradimer coupling [$J_0 = 2.38(2)$ meV] and weak interdimer couplings less than 0.52(2) meV. Thus, $Ba_3Cr_2O_8$ provides a new testing ground for theories of the condensation of magnons.

Two single crystals of $Ba_3Cr_2O_8$ with weights of 280 mg and 170 mg that were grown by the floating zone method were comounted in the (hhl) scattering plane for inelastic neutron scattering measurements, while the larger crystal was later mounted in the ($h0l$) plane for elastic measurements. All measurements on the crystals were performed at the cold-neutron triple-axis spectrometer, located at the NIST Center for Neutron Research (NCNR). For inelastic measurements, the crystals were cooled in a liquid ^{4}He cryostat for the measurement without a field, and in a 11.5 T superconducting magnet for the field measurements, while for the elastic measurements the crystal was inside a 4 K closed-cycle refrigerator (displex). For the inelastic measurements, a horizontally focusing analyzer mode was utilized to cover the scattering angle of about 5 degrees at a time, while for the elastic measurements conventional horizontal collimations of open-80′-80′-open. For both measurements, the energy of the scattered neutrons was set to $E_f = 5$ meV, and a liquid nitrogen cooled Be filter was placed before the analyzer to eliminate high order neutron contaminations. Neutron powder diffraction measurements were also performed on a 15 g powder sample inside a 4 K displex at the BT1 neutron powder diffractometer at NCNR, using a Ge311 monochromator.

In order to investigate the intra- and interdimer interactions in $Ba_3Cr_2O_8$, we have performed inelastic neutron scattering measurements on single crystals at 1.7 K. Several constant $\boldsymbol{Q}$ scans were performed to map the dispersion of the singlet-to-triplet excitations. Figure 2 shows the results along three high symmetry directions. Along the (0, 0, l) direction, a nearly flat excitation mode centered ~2 meV is observed with a bandwidth of ~0.7 meV [see Fig. 2(a)]. This dispersion is due to the weak interdimer interactions, J_1 and J_4, between the dimer planes (see Fig. 1). The (h, h, 3) and (h, h, $3h$) directions, which probe the interplane interdimer interactions, J_2, J_3, as well as the out-of-plane ones, show three unexpected excitation modes [see Figs. 2(b) and 2(c)]. In contrast, $Ba_3Mn_2O_8$ displays only a single triplet excitation along all the symmetric directions measured [12]. Magnetic excitations from weakly coupled dimer systems can be well explained within the random phase approximation that gives the dispersion relation [12–14] $\hbar\omega(\boldsymbol{Q}) \simeq \sqrt{J_0^2 + J_0\gamma(\boldsymbol{Q})}$, where $\gamma(\boldsymbol{Q}) = \sum_i J(\boldsymbol{R}_i)e^{-i\boldsymbol{Q}\cdot\boldsymbol{R}_i}$ and $J(\boldsymbol{R}_i)$ represents interdimer interactions. If the interdimer interactions are spatially isotropic, as shown in Fig. 1(a), then the four nearest interactions, J_1, J_2, J_3, J_4, give

$$\begin{aligned}\gamma(\boldsymbol{Q}) = {} & 2J_1[\cos\{\tfrac{2}{3}\pi(2h+k+l)\} + \cos\{\tfrac{2}{3}\pi(-h+k+l)\} \\ & + \cos\{\tfrac{2}{3}\pi(-h-2k+l)\}] + 2(J_2 - J3)[\cos\{2\pi h\} \\ & + \cos\{2\pi k\} + \cos\{2\pi(h+k)\}] \\ & + 2J_4[\cos\{\tfrac{2}{3}\pi(2h+4k+l)\} + \cos\{\tfrac{2}{3}\pi(2h-2k+l)\} \\ & + \cos\{\tfrac{2}{3}\pi(-4h-2k+l)\}],\end{aligned}$$

such that without a field only a single triplet excitation along any of the (h, h, l) directions is expected, as recently observed in the related $s = 1$ system $Ba_3Mn_2O_8$ [12].

What is the origin of the complex excitations observed in $Ba_3Cr_2O_8$? One possibility would be that the triply degenerate singlet-to-triplet excitation mode is already split into three modes in the (h, h, l) scans as a result of single anisotropy terms. If this is the case, then each excitation in the (h, h, l) scan are not degenerate and therefore remain single under an application of an external magnetic field. This conjecture was tested by performing further inelastic neutron experiments at constant $\boldsymbol{Q}$ under an external magnetic field, which are shown in Fig. 3. In Fig. 3(a), the single mode at $\boldsymbol{Q} = (0, 0, 4.5)$ at $H = 0$ T splits into three modes for finite values of a field. As H increases, the Zeeman energy splitting increases as expected. Furthermore, Fig. 3(b) shows the two strong modes at $\boldsymbol{Q} = (0.5, 0.5, 3)$ that appeared at $\hbar\omega = 1.4$ meV and 3.05 meV without a field also revert to three modes when H

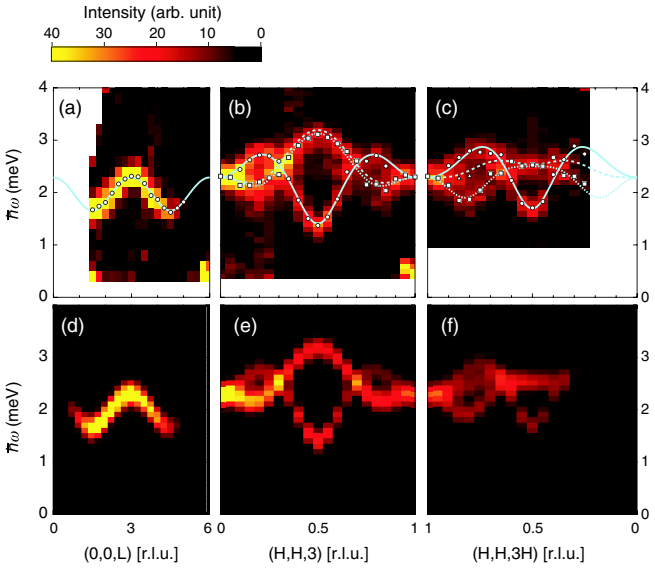

FIG. 2 (color online). Contour maps of dispersion relations along (a) (0, 0, l), (b) (h, h, 3), and (c) (h, h, $3h$) directions. The data were taken by performing constant $\boldsymbol{Q}$ scans of $Ba_3Cr_2O_8$ single crystals at 1.7 K. The point symbols represent the peak positions obtained by fitting the data with simple Gaussians. (d), (e) Calculated dispersions and intensities based on a model of spatially anisotropic interdimer interactions, which is described in the text.

is applied. This demonstrates unambiguously that both modes are triply degenerate singlet-to-triplet excitations.

Another possibility is that, in analogy to the acoustic and optical vibrational modes that exist in a lattice with more than one ion in a unit cell, the origin might be an acoustic and two optical magnon modes as a result of the three bilayers in the chemical unit cell. Such an optical magnon mode has been observed in $Cs_3Cr_2Br_9$, where $Cr^{3+}(3d^3; s = 3/2)$ ions form two bilayer triangular planes [13]. The optical mode, however, appeared along certain symmetry directions with much weaker intensity than the acoustic mode. For $Cs_3Cr_2Br_9$, Leuenberger *et al.* have calculated, using a Green's function technique, the dispersions and intensities of the acoustic and optical modes. They showed that the intensity of the acoustic mode is proportional to $1 + \cos(\boldsymbol{\rho} \cdot \boldsymbol{\tau} + \phi)$, while that of the optical mode is related to $1 - \cos(\boldsymbol{\rho} \cdot \boldsymbol{\tau} + \phi)$ where $\boldsymbol{\rho}$ is the displacement vector between two different sublattices (planes), $\boldsymbol{\tau}$ a reciprocal lattice vector, and ϕ is the phase of the Fourier sum of the interplane interactions which is complex in the case of $Cs_3Cr_2Br_9$ [13]. Their calculations were consistent with their data. We have implemented their model for the present case, $Ba_3Cr_2O_8$, which suggests the presence of one acoustic and two optical modes. However, for this case ϕ turns out to be zero because of the inversion symmetry at the center of the dimer, and therefore the Fourier sum of the interplane interactions becomes real. Since $\boldsymbol{\tau}(h, k, l)$ must satisfy the reflection condition $-h + k + l = 3n$ with an integer n for the $R\bar{3}m$ symmetry and $\boldsymbol{\rho} = (\frac{2}{3}, \frac{1}{3}, \frac{1}{3})$, $\cos(\boldsymbol{\rho} \cdot \boldsymbol{\tau})$ is always 1. Therefore, the optical modes in $Ba_3Cr_2O_8$ are not present, and the observed excitations are all acoustic in nature, which is consistent with the observation of only one single triplet mode in the related compound $Ba_3Mn_2O_8$ [12].

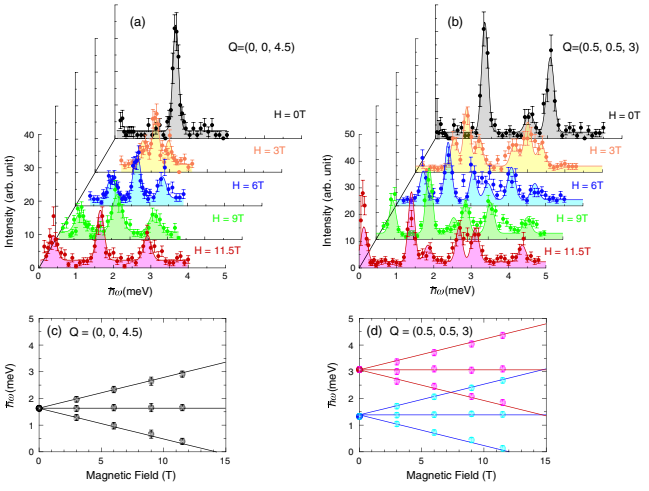

FIG. 3 (color online). Constant $\boldsymbol{Q}$ scan with several different magnetic fields (H) (a) at $\boldsymbol{Q} = (0, 0, 4.5)$ and (b) at $\boldsymbol{Q} = (0.5, 0.5, 3)$ scan, and H dependence of the peak positions in $\hbar\omega$ (c) at $\boldsymbol{Q} = (0, 0, 4.5)$ and (d) at $\boldsymbol{Q} = (0.5, 0.5, 3)$. The lines represent the Zeeman splitting.

A third possibility is that the interdimer interactions are not spatially isotropic and the three modes arise from three different crystal domains. To test this scenario, we have considered a set of spatially anisotropic interdimer interactions, J_1', J_1'', J_1''', J_2', J_2'', J_2''', J_4', J_4'', J_4''', as depicted in Fig. 1(c). J_3 is neglected because we cannot observe J_3 separately but we only observe $J_2 - J_3$. Then, for one crystal domain

$$\begin{aligned}\gamma(h, h, l) = {} & 2J_1' \cos\{\tfrac{2}{3}\pi(3h + l)\} + 2J_1'' \cos\{\tfrac{2}{3}\pi l\} \\ & + 2J_1''' \cos\{\tfrac{2}{3}\pi(-3h + l)\} + 2(2J_2'' + 2J_2''') \\ & \times \cos\{2\pi h\} + 2J_2''' \cos\{4\pi h\} \\ & + 2J_4' \cos\{\tfrac{2}{3}\pi(-6h + l)\} + 2J_4'' \cos\{\tfrac{2}{3}\pi l\} \\ & + 2J_4''' \cos\{\tfrac{2}{3}\pi(6h + l)\}.\end{aligned}$$

For the other two domains, the coupling constants are permuted: $\{J'_{1,2,4}, J''_{1,2,4}, J'''_{1,2,4}\} \rightarrow \{J''_{1,2,4}, J'''_{1,2,4}, J'_{1,2,4}\} \rightarrow \{J'''_{1,2,4}, J'_{1,2,4}, J''_{1,2,4}\}$. This suggests that three domains will produce the same dispersion along the (0, 0, l) direction, whereas along the (h, h, 3) and (h, h, 3h) directions each domain will yield a unique dispersion as shown in different lines in Figs. 2(b) and 2(c). Figures 2(d)–2(f) are calculated dispersion relations and demonstrate that the experimental data can be simulated by this model when $J_0 = 2.38(1)$, $J_1' = 0.08(2)$, $J_1'' = -0.15(2)$, $J_1''' = 0.10(1)$, $J_2' = 0.10(2)$, $J_2'' = 0.07(2)$, $J_2''' = -0.52(2)$, $J_4' = 0.04(2)$, $J_4'' = 0.10(2)$, $J_4''' = 0.09(2)$. All values are given in meV.

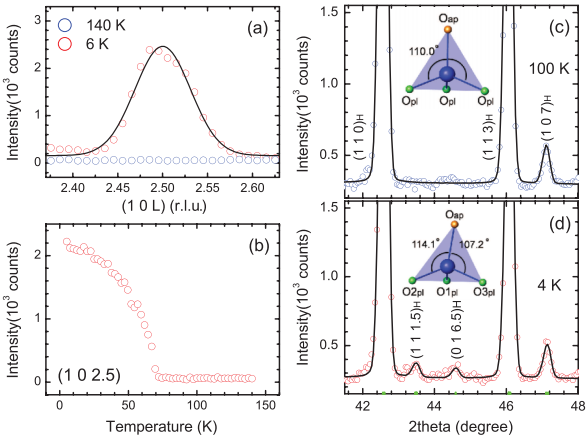

FIG. 4 (color online). Elastic neutron scattering data obtained from a single crystal of $Ba_3Cr_2O_8$, (a) as a function of the wave vector at 140 K (blue, or dark, circles) and 6 K (red, or light, circles) and (b) as a function of temperature that shows the (1, 0, 2.5) superlattice peak appears below 70 K. (c), (d) Neutron diffraction data obtained from a powder sample at two different temperatures, 100 K and 4 K. The line in (a) is fit to a Gaussian, while the lines in (c) and (d) are the results of the crystal refinements using Rietveld analysis based on $R\bar{3}m$ and $C2/c$ symmetry, respectively. The nuclear Bragg peaks are indexed in terms of the hexagonal lattice parameters for convenience. Insets in (c) and (d) show the local oxygen environment in each phase.

TABLE I. The refined crystal structural parameters of $Ba_3Cr_2O_8$ at 4 K and 100 K, using FULLPROF. The symmetry was found to be $R\bar{3}m$ at 100 K and $C2/c$ at 4 K. W represents the crystallographic Wyckoff position, $\chi^2 = \sum_i \{I_{\mathrm{obs},i} - I_{\mathrm{cal},i}\}^2/\Delta I^2_{\mathrm{obs},i}$ and $R_{F^2} = 100 \times \sum_{h,k,l}|I_{\mathrm{obs}}(h,k,l) - I_{\mathrm{cal}}(h,k,l)|/\sum_{h,k,l}|I_{\mathrm{obs}}(h,k,l)|$ where I_{obs} and I_{cal} are the observed and calculated intensity, respectively.

Atom (W)	x	y	z	B_{iso}(Å^2)
100 K ($R\bar{3}m$), $\chi^2 = 1.92$, $R_{F^2} = 2.55$				
$a = b = 5.724\,78(7)$ Å, $c = 21.378\,83(27)$ Å				
Ba1(3a)	0	0	0	0.429(46)
Ba2(6c)	0	0	0.205 81(7)	0.071(29)
Cr(6c)	0	0	0.407 18(8)	0.083(45)
$O_{pl}(18h)$	0.828 51(8)	0.171 49(8)	0.898 75(3)	0.546(24)
$O_{ap}(6c)$	0	0	0.328 62(6)	1.398(34)
4 K ($C2/c$), $\chi^2 = 1.64$, $R_{F^2} = 2.58$				
$a = 9.905\,36(25)$ Å, $b = 5.725\,46(14)$ Å, $c = 14.628\,93(22)$ Å				
$\beta = 103.115\,26(226)°$				
Ba1(4e)	0	0.265 22(73)	0.25	0.272(49)
Ba2(8f)	0.100 45(55)	0.249 88(57)	0.558 56(10)	0.008(29)
Cr(8f)	0.201 35(80)	0.251 09(73)	0.860 54(12)	0.089(46)
$O1_{pl}(8f)$	−0.119 98(46)	0.253 28(92)	0.400 35(41)	0.422(24)
$O2_{pl}(8f)$	0.134 43(62)	−0.009 34(81)	0.400 18(32)	0.422(24)
$O3_{pl}(8f)$	0.139 74(61)	0.506 90(77)	0.405 29(27)	0.422(24)
$O_{ap}(8f)$	0.161 67(47)	0.278 93(56)	0.742 87(9)	0.907(39)

Now what is the origin of the spatially anisotropic interdimer exchange interactions in $Ba_3Cr_2O_8$? In order to address this issue, we have performed elastic neutron scattering measurements on a single crystal to search for superlattice peaks linked to possible lattice distortions. Figures 4(a) and 4(b) show that a nuclear superlattice peak at (1, 0, 2.5) develops in a second order fashion below 70 K. The appearance of the superlattice peak clearly indicates that the rhombohedral $R\bar{3}m$ crystal structure symmetry at room temperature is lowered to the monoclinic $C2/c$ symmetry at low temperatures. To refine the crystal structure, we performed neutron diffraction measurements on a powder sample at 100 K and 4 K [see Figs. 4(c) and 4(d)]. Table I lists the structural parameters optimized by Rietveld analysis, and the insets of 4(c) and 4(d) and show changes of the local oxygen environment. In the $R\bar{3}m$ symmetry, the apical oxygen (O_{ap}) lies exactly above the chromium ion and is symmetrically positioned with respect to the neighboring CrO_4 tetrahedra in the triangular plane. However, in the $C2/c$ symmetry, the apical oxygen moves away from the high symmetry position in the triangular plane and induces the spatially anisotropic interactions between dimers. A similar lattice distortion was recently observed in a powder sample of $Sr_3Cr_2O_8$ [15]. We expect that $Sr_3Cr_2O_8$ would also exhibit more than one single triplet excitation mode without a field, as was very recently confirmed by inelastic neutron scattering measurements on a single crystal of $Sr_3Cr_2O_8$ [16]. In comparison, $Ba_3Mn_2O_8$ lacks orbital degeneracy, and thus has spatially isotropic J's that leads to the single triplet excitations as observed in Ref. [12].

In summary, the triplet excitations in the spin gap system, $Ba_3Cr_2O_8$, are measured by inelastic neutron scattering on single crystals, while its crystal structure is determined from neutron diffraction experiments. The combination of these results shows that $Ba_3Cr_2O_8$ is a good model system for weakly coupled $s = 1/2$ quantum spin dimers with the intradimer coupling of $J_0 = 2.38(2)$ meV and the interdimer couplings less than 0.52 (2) meV, which are spatially anisotropic due to lattice distortions induced by the Jahn-Teller active Cr^{5+} ions.

We thank A. Lamacraft, D. Khomskii, M. V. Mostovoy, C. D. Batista, S. Hass, and S. Ishihara for helpful discussions. Work at the University of Virginia and NCNR was supported by the U.S. DOE through DE-FG02-07ER46384 and the U.S. NSF through DMR-0454672, respectively. S. J. is partially supported by the U.S. DOC-NIST through 70NANB7H6035.

[1] S. Sachdev, Nature Phys. **4**, 173 (2008).
[2] T. Nikuni *et al.*, Phys. Rev. Lett. **84**, 5868 (2000).
[3] H. Tanaka *et al.*, J. Phys. Soc. Jpn. **70**, 939 (2001).
[4] Ch. Rüegg *et al.*, Nature (London) **423**, 62 (2003).
[5] S. E. Sebastian *et al.*, Nature (London) **441**, 617 (2006).
[6] T. Giamarchi *et al.*, Phys. Rev. B **59**, 11 398 (1999).
[7] M. Matsumoto *et al.*, Phys. Rev. Lett. **89**, 077203 (2002).
[8] M. Uchida *et al.*, J. Phys. Soc. Jpn. **70**, 1790 (2001).
[9] H. Tsujii *et al.*, Phys. Rev. B **72**, 214434 (2005).
[10] T. Nakajima *et al.*, J. Phys. Soc. Jpn. **75**, 054706 (2006).
[11] Y. Singh *et al.*, Phys. Rev. B **76**, 012407 (2007).
[12] M. B. Stone *et al.*, Phys. Rev. Lett. **100**, 237201 (2008).
[13] B. Leuenberger *et al.*, Phys. Rev. B **30**, 6300 (1984).
[14] N. Cavadini *et al.* Eur. Phys. J. B **7**, 519 (1999).
[15] L. C. Chapon *et al.* arXiv:cond-mat/0807.0877.
[16] B. Lake (private communication).